

Magnetic Behaviour of Er and Mg Doped Bismuth Ferrite Nanocomposites: Synthesis and Its Characterization

Thirumoorthi. A

Associate Professor, Department of Chemistry, Government Arts College, Udumalpet – 642 126, Tamilnadu, India

Abstract

Multiferroic materials have significant attention due to the coupled magnetic, ferro- electric and ferro-elastic orders. Among all multiferroic materials, bismuth ferrites (BiFeO_3 , BFO) are the only single-phase room temperature multiferroic materials known, and have multifunctional applications. Bismuth ferrite possesses magnetic ordering of antiferromagnetic with a spatially modulated spin structure. Consequently, many researchers are engaged in releasing the ferromagnetism from space-modulated spin structure. This paper provides insights into the synthesis and characterization of Er^{3+} and Mg^{2+} co-doped single-phase BFO nanocomposites namely BEFO, BEFMO-1 and BEFMO-2 with different mole ratios of magnesium by sol-gel method. FT – IR spectra confirmed the presence of Bi/Er –O bonds in doped BFO and the Raman spectra indicates the structural transformation of rhombohedral to orthorhombic. SEM images showed the undoped and doped BFO nanocomposites synthesized were spherical in shape and PL studies revealed that the reduction in the density of oxygen vacancies causing decrease in electron-hole recombination. Bismuth ferrites provide enhanced magnetic (M_s , M_r and H_c) behaviours due to doping of Er and Mg.

Keywords: Bismuth ferrites; Er and Mg doping; Magnetic Hysteresis; PL studies.

1. Introduction

Recently, nanocomposite materials have pulled in the attention, imagination and close scrutiny of scientists and engineers. This results from the simple premise that using building blocks with dimensions in the nano sized range which makes it possible to design and create new materials with unprecedented improvements in their physical properties. This ability to tailor composites by using nano size building blocks of heterogeneous chemical species has been demonstrated in several interdisciplinary fields. The constituents of a nanocomposite have different structures and compositions and hence unusual properties, they serve various functions. Thus, the materials built from them can be multifunctional. Also, nanocomposites offer useful new properties compared to conventional materials.

Multiferroic $\text{Bi}_{1-x}\text{Gd}_x\text{FeO}_3$ ceramics ($x = 0.0, 0.05$ and 0.10) have been synthesized by Sujata Sanghi et al. via two stage solid-state reaction method [1]. The structure phase transition from rhombohedral (R3c) to orthorhombic (Pnma) at $x \geq 0.10$ was observed by XRD and Rietveld analysis. An increase in magnetization and coercive field was observed by the replacement of Fe^{3+} with Gd^{3+} . The improvement

in dielectric parameters and magnetic property is due to the presence of structural transformation of BFO lattice by incorporating Gd.

Pal et al. prepared the enhanced magnetic, electric and magneto-dielectric (MD) properties of BFO by gadolinium doping through sol-gel method. The phase-purity and nanocrystalline nature of the samples have been confirmed by the XRD and TEM measurements. Both dc and ac electrical properties were measured to understand the charge transport mechanism. The dc electrical resistivity was found due to a variable range hopping conduction mechanism. The variation of ac-conductivity is based on the correlated barrier hopping (CBH) conduction mechanism. The improved magnetic and electrical properties have been attributed to a possible suppression of the inhomogeneous magnetic spin structure and broken periodicity of the spin cycloid of BFO owing to smaller crystallite size and decrease of the oxygen vacancies [2].

Pure BiFeO₃ (BFO), Dy doped BiFeO₃ (BDFO) and Dy-Mn co-doped BiFeO₃ (BDFMO) thin films were successfully prepared on SnO₂: F (FTO)/glass substrates by a sol-gel method. A structural transition from the trigonal structure (R3c: H) to the trigonal structure (R3m: R) was observed in the Dy doped and Dy-Mn co-doped BFO thin films by XRD, Rietveld refinement and Raman spectra. The results illustrated the high multiferroic property, giant remanent polarization and a relatively large saturation magnetization of BDFMO thin films [3]. Single-phase Bi_{0.95}Ln_{0.05}Fe_{0.95}Co_{0.05}O₃ (Ln= La, Pr) nanoparticles were prepared by Weiwei Mao et al. through sol-gel method [4]. The impurity phase was effectively suppressed and the magnetic properties of two co-doped samples were significantly enhanced. The significant structure distortion of Fe-O bonds due to high value of saturated magnetization, the co-doping of La and Co into BFO reduced the leakage current and enhanced the ferroelectric properties observed from Raman spectra.

Gadolinium (Gd) and Dysprosium (Dy) doped multiferroic BGM and BFM ceramics has been synthesized by solid state reaction (SSR) technique. The crystal structure of the ceramic samples showed a monoclinic phase. The studies of dielectric properties like dielectric constant (ϵ) and loss tangent ($\tan\delta$) suggested ferroelectric-para electric phase transition in the compounds. The vibrating sample magnetometer (VSM) measurement showed a significant change in the magnetic properties of Gd and Dy doped samples [5]. Bi_{1-x}Pr_xFe_{1-x}Ti_xO₃ ceramics with $x \leq 0.20$ were synthesized by solid state reaction method [6]. The single phase formation of all samples were observed in XRD and the structural transition from rhombohedral (R3c) phase for $x \leq 0.10$ to orthorhombic (Pnma) phase for $x \geq 0.15$ was observed by Rietveld refinement of diffraction data. The dielectric properties of samples were improved by controlling the amount of co-doping. M-H measurements showed an increase in magnetization with x due to the partial destruction of spin cycloid of Fe-O-Fe network caused by Ti doping. Absorption of light in the range of 520-546 nm indicates an optical band gap in the visible range for these doped materials.

Ahmed et al. prepared nanometric multiferroic sample of Bi_{1-x}La_xFeO₃ ($0.05 < x < 0.40$) using ceramic method [7]. The decrease in the lattice parameters was due to the difference in the ionic radii of Bi and La and this effect was compensated by change in the atomic weight of the two elements. All samples of the ceramics showed anti-ferromagnetic and the small values of remnant and saturation magnetization indicated the canted type anti-ferromagnetism. The magnetic susceptibility measurements showed its size dependence due to long range spin arrangement. Improved magnetization of BiFeO₃ is achieved by La³⁺ at different doping levels. Garg et al. [8] reported that the preparation of Pure and Samarium (Sm) doped BiFeO₃ through a solid state reaction method. At a calcination temperature of 825°C, undoped

samples were found that maximum amount of pure phase BiFeO_3 , whereas a deviation in calcination temperature leads to secondary phases such as $\text{Bi}_{25}\text{FeO}_{40}$. On the other hand, Sm doped BiFeO_3 samples revealed that the secondary phases do not appear on calcination at above 800°C . Vibrating sample magnetometry (VSM) measurements showed that $\text{Bi}_{0.9}\text{Sm}_{0.1}\text{FeO}_3$ samples possessed higher remnant magnetization than undoped samples. Ferroelectric measurement showed that Sm doping in BiFeO_3 improves the polarization, but at the same time it enhances the leakage current.

Pure phase and $\text{Sm}^{3+}/\text{Zr}^{4+}$ co-doped BiFeO_3 through sonochemical method were synthesized by Dimple P. Dutta et al. [9]. The presence of the dopant ions have been established by energy dispersive spectroscopy (EDS) and X-ray photoelectron spectroscopy (XPS). It has been found that $\text{Sm}^{3+}/\text{Zr}^{4+}$ doped BiFeO_3 shows the ferromagnetism while the bulk BiFeO_3 shows anti-ferromagnetic behaviour due to size effects and lattice distortions in the sample. Also, doping decreases the leakage current and improves its ferroelectric properties and the suppression of oxygen vacancy is related to defect more effective with Sm^{3+} doping in Bi^{3+} site compared to acceptor doping of Zr^{4+} in Fe^{3+} site of BiFeO_3 . The enhanced magneto dielectric properties in the $\text{Sm}^{3+}/\text{Zr}^{4+}$ doped BiFeO_3 suggested that these materials are used in memory storage devices.

Yu Sui prepared single phase Europium doped BFO multiferroic ceramics to study the effects of Eu substitution on their crystal structure and ferroelectromagnetic behaviour of $\text{Bi}_{1-x}\text{Eu}_x\text{FeO}_3$ ($0 \leq x \leq 0.3$) [10]. The XRD studies revealed that a structural phase transitions $\text{R3c} \rightarrow \text{Pn}2_1\text{a}$ occurs at $x = 0.2$. Europium substitution effectively induced the appearance of spontaneous magnetization and enhanced composition-driven transition from a rhombohedral to an orthorhombic phase. By increasing Eu concentration, the leakage current was found to be reduced. The electric hysteresis loops of $\text{Bi}_{1-x}\text{Eu}_x\text{FeO}_3$ ceramics were obtained and the loops were not saturated.

The systematic studies of crystalline structure, magnetic and ferroelectric properties of La and Pr doped polycrystalline $\text{Bi}_{1-x-y}\text{La}_x\text{Pr}_y\text{FeO}_3$ ceramic samples have been done by Srivastava et al. [11]. La and Pr substitution at Bi site eliminates the impurity phases in the doped ceramic samples completely. Rietveld refinement showed that the crystal structure changes from Rhombohedral (R3c) to Orthorhombic (pbnm) with increased concentration of La and Pr. Substantial enhancement in magnetization of $\text{Bi}_{1-x-y}\text{La}_x\text{Pr}_y\text{FeO}_3$ has been observed and the structural phase change with doping of Pr leads to the suppression of helical spin order. It has been found that the dielectric constant and dielectric loss get improved by La and Pr co-substitution. The improvement in dielectric properties is due to the changes in lattice parameters and suppression of oxygen vacancies caused by La and Pr co-substitution.

Polycrystalline $\text{Bi}_{1-x}\text{Dy}_x\text{FeO}_3$ ($x=0.03, 0.05, 0.07, 0.10$ and 0.12) ceramics has been synthesized by solid state reaction route and the Rietveld refinement revealed that all the samples crystallize in the rhombohedral structure with non-centrosymmetric R3c space group. Substitution induced suppression of the spiral spin structure and $\text{Dy}^{3+} - \text{Fe}^{3+}$ interaction enhanced RT magnetization. The magnetic coupling between $\text{Dy}^{3+} - \text{Fe}^{3+}$ and $\text{Dy}^{3+} - \text{Fe}^{3+}$ ions enhanced at low temperatures range for $x = 0.07 - 0.12$ samples and the dielectric properties were improved with increasing Dy content in BiFeO_3 [12].

Xingsen Gao et al. prepared Mg doped $\text{Bi}_{0.8}\text{Ca}_{0.2}\text{FeO}_3$ ceramics and studied the structural and enhanced ferromagnetic properties. Oxygen vacancies are introduced into $\text{Bi}_{0.8}\text{Ca}_{0.2}\text{Fe}_{1-x}\text{Mg}_x\text{O}_3$ ceramics by doping in order to induce the enhanced macroscopic ferromagnetism from anti-ferromagnetism. The enhanced ferromagnetism is due to the creation of unbalanced Fe^{3+} spins induced by the collapse of the space modulated cycloidal spin structure and relative long-range coupling mediated by the oxygen vacancies trapped localized electrons [13].

Yang et al. reported that Mn and Mg co-doped BiFeO₃ films have been developed on Si (100) substrates by sol-gel method [14]. Rhombohedral lattice structure and phase transition was confirmed by XRD and Raman spectra. The improved surface morphology and decreased grain size of films were due to the influence of Mn and Mg co-doping which was observed in SEM. In Photoluminescence spectra, a blue emission of xBFMMO films was found while the non-linear shift of emission peaks indicates the variation of band gap. M-H curves exhibits the enhanced saturation magnetization due to destroyed spin cycloid and released locked magnetization. This offers a great potential on the multiferroic information storage applications.

Recently, the research interest in multiferroic materials, in which ferroelectricity, ferroelasticity and ferromagnetism coexist, has increased due to the multifunctional device applications. BiFeO₃ with distorted rhombohedral perovskite structure is the most interesting multiferroic compound, provides an enormous potential for technological applications and hence the present study.

2. Materials and Methods

Nano-sized composites of Bi_{0.8}Er_{0.2}Fe₁Mg₀O₃ (BEFO), Bi_{0.8}Er_{0.2}Fe_{0.9}Mg_{0.1}O₃ (BEFMO-1) and Bi_{0.8}Er_{0.2}Fe_{0.8}Mg_{0.2}O₃ (BEFMO-2) were synthesized via sol-gel method. The appropriate proportions of analar grade of Bismuth nitrate [Bi(NO₃)₃.5H₂O, 98%], iron nitrate [Fe(NO₃)₃.9H₂O, 98%], Erbium nitrate [Er(NO₃)₃.5H₂O, 99.9%] and Magnesium nitrate [Mg(NO₃)₂.6H₂O, 99%] were used as starting materials and dissolved in 1.2 mL of nitric acid (99.5%) and double distilled water. Ascorbic acid was added as an organic complex to the reaction mixture. After the dissolution of the reactants completely, the solution was stirred for 1 to 2 hours to attain a homogeneous gel like mass and dried. Further, the dried samples were underwent thermal treatment at 250°C and 800°C for 1hour [15].

3. Results and Discussion

3.1 UV – Visible spectra

The UV-Visible absorption spectra and the corresponding Tauc's plot for the Er and Mg co-doped BFO samples are shown in Figure: 1 (a) and (b). A strong band is observed around the wavelength of 450 nm is attributed to metal-metal transition and the weak band in the range of 600–700 nm is assigned to the crystal field transition. The direct band gap is calculated using Tauc's equation by plotting $[\alpha h\nu]^2$ as a function of energy and is equal to zero. The estimated band gap is found to be 2.23, 2.10 and 1.89 eV for BEFO, BEFMO-1 and BEFMO-2 samples with absorption maximum at 417, 427 and 448nm respectively. The observed changes in band gap energy may due to the size effect and the structural distortion induced in the host materials. In particular, co-substitution of Er in BFO induces change in Fe-O-Fe bond angles due to octahedral distortion. Thus, the narrow optical energy band gap value obtained suggests that Er doped BFO samples would be a potential candidate towards the application of visible light photocatalyst.

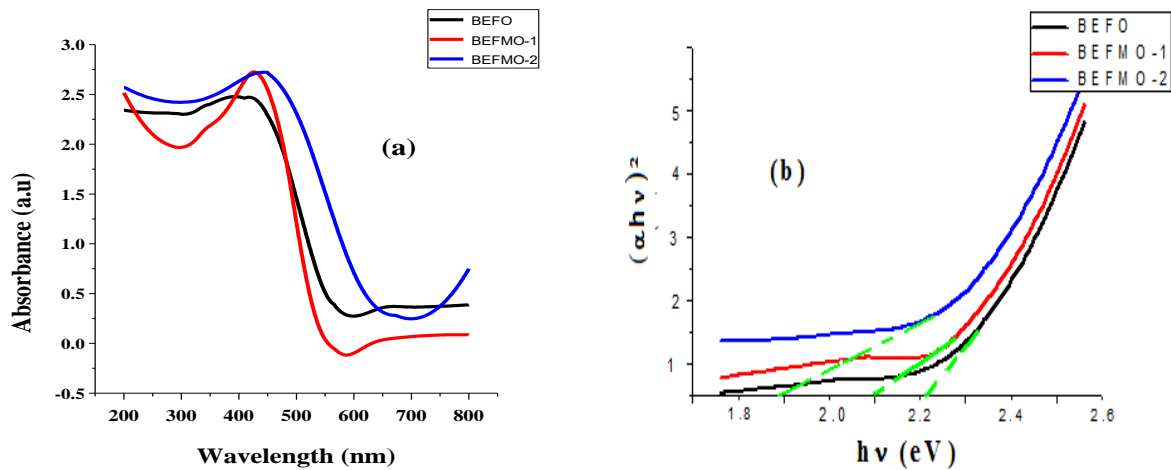


Figure 1: (a) UV- Visible spectra

(b) Tauc's plot

3.2 FT – IR spectra

Figure: 2 shows the FT-IR spectra of doped bismuth ferrite nanocomposites. The FT-IR spectra of BEFO show a peak at 589.89 cm^{-1} due to Bi/Er-O vibration mode. The vibration mode of Mg doped composites has been shifted to lower values of 588.31 and 583.49 cm^{-1} corresponding to BEFMO-1 and BEFMO-2 respectively. Since bending of Fe-O and Bi-O bonds developed due to the deformation of octahedron with Er and Mg substitution and also the bending of OH bonds in water molecule decreases with increase in concentration of dopants.

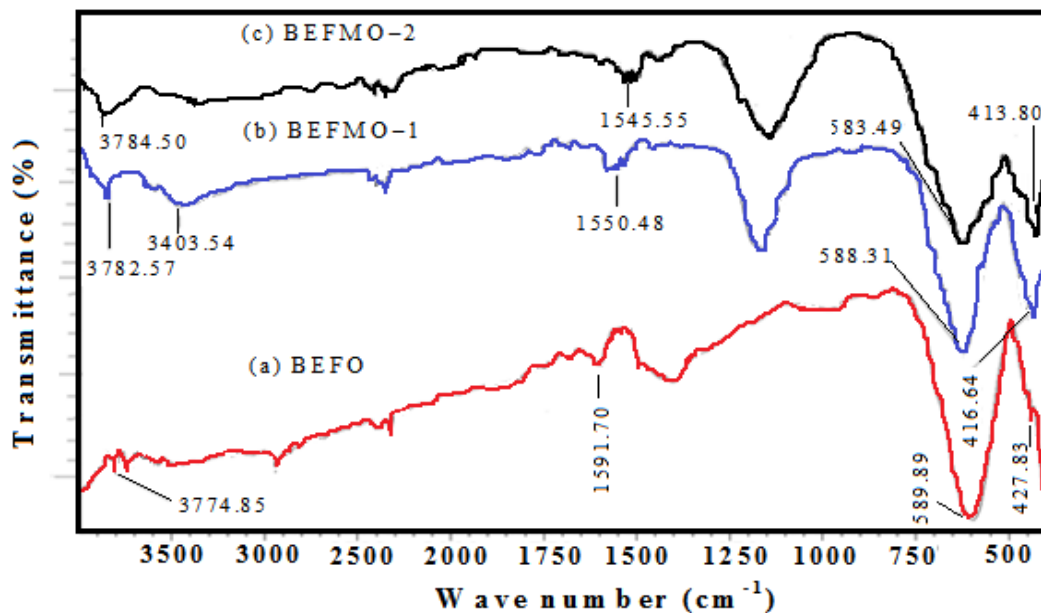


Figure: 2 FT – IR spectra

3.3 XRD studies

The XRD pattern of BEFO, BEFMO-1 and BEFMO-2 nanocomposites synthesized are shown in figure: 3. The pure, undoped BFO depicts the rhombohedral symmetry which involves in structural distortion and hence transformed to orthorhombic (lbmm) symmetry by dopants. The structural distortion was attributed as a result of small ionic radius of Er^{3+} (0.89 \AA) in comparison with that of Bi^{3+} (1.03 \AA).

The peaks in the XRD are indexed as (130), (121), (200), (141), (150), (210), (042), (202), (242), (280), (143), (1 10 1) and (1 11 1) shown in figure: 3(c). Although, further doping of magnesium (Mg^{2+}) in B site of Fe^{3+} (0.645 \AA) does not change the existing structure, the increase in atomic number of the transition elements leads to a reduction in ‘b’ parameter eventually the cell volume changes due to the variation of ionic radius of Mg^{2+} (0.66 \AA).

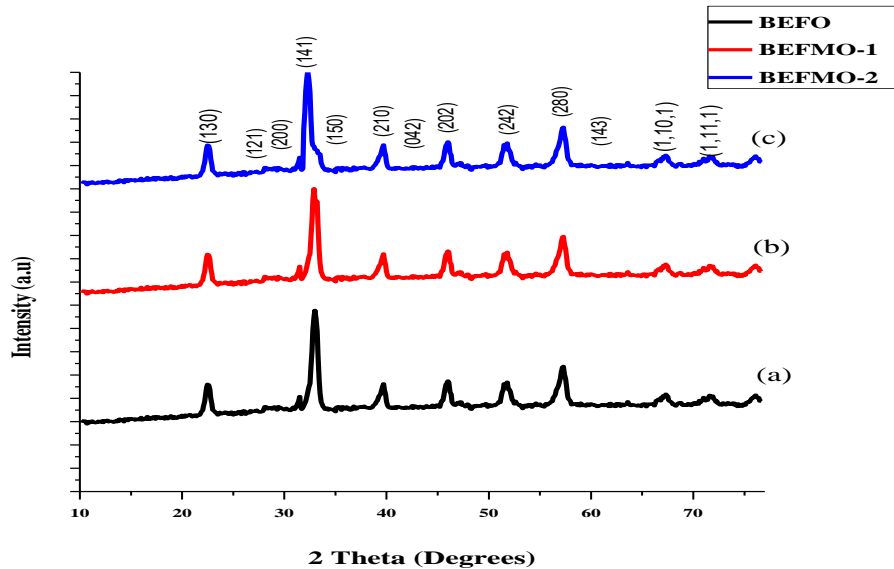


Figure: 3 XRD

The Goldschmidt tolerance factor determines the distortion degree of ABO_3 perovskite and the stability of perovskite compounds is based on ABO_3 formula. The reduction of tolerance factor for BEFO, BEFMO-1 and BEFMO-2 nanocomposites are owing to the variation of average radius at A site or B site, indicating that $Fe^{3+}/Mg^{2+}-O$ and $Bi^{3+}/Er^{3+}-O$ bonds are under the compression and tension forces respectively. In order to reduce the lattice stress after doping Er^{3+} and Mg^{2+} , oxygen octahedron rotates cooperatively which leads to the transformation of crystal structure of $BiFeO_3$ with the substitution of Er^{3+} and Mg^{2+} . Thus, the change in Goldschmidt tolerance factor values further proved that the substitution of Er^{3+} and Mg^{2+} results in the transformation of crystal structure from rhombohedral to orthorhombic phase [16]. The following table 1 gives the crystallographic parameters of doped BFO nanocomposites.

Table 1: Crystallographic parameters of Er^{3+} and Mg^{2+} co-doped BFO nanocomposites:

Compounds	a (\AA)	b (\AA)	c (\AA)	Cell volume V (\AA^3)	Crystalline size (nm)	Tolerance factor
$Bi_{0.9}Er_{0.1}FeO_3$	5.5898	15.7286	5.6121	493.4	64.5	0.8351
$Bi_{0.9}Er_{0.1}Fe_{0.9}Mg_{0.1}O_3$	5.5482	15.5159	5.4372	468.1	52.6	0.8344
$Bi_{0.9}Er_{0.1}Fe_{0.8}Mg_{0.2}O_3$	5.5276	15.3293	5.5470	470.1	21.7	0.8338

3.4 Raman spectra

Figure: 4 shows the Raman spectra of BEFO, BEFMO–1 and BEFMO–2 nanocomposites. The ionic radius of Er^{3+} (0.89 \AA) is smaller than that of Bi^{3+} (1.03 \AA) and hence, it is easy to substitute Er into the

Bi site of BFO. The changes observed in the low frequency Raman modes (A_1) for the synthesized nanocomposites are mainly due to the Er substitution into the Bi site of the perovskite BFO. The low frequency modes move towards a higher frequency, which associated with the reduction of activity of Er doped in BFO. After co-doping of Mg^{2+} ($(0.66A^\circ)$ ions), the A and E modes changed in which the E-mode regarded as the bending and stretching of FeO_6 octahedra. The A_1-1 mode of intensity is reduced to 280, 240, 190 counts for BEFO, BEFMO –1 and BEFMO –2 respectively and the significant changes in E modes shifted towards higher wave numbers with intensity enhancement indicating that the structural transformation from rhombohedral to orthorhombic occurs which altered the Fe–O bonds by doping Mg^{2+} ions [16,17]. The comparison of E mode intensities of doped nanocomposites are given in table 2.

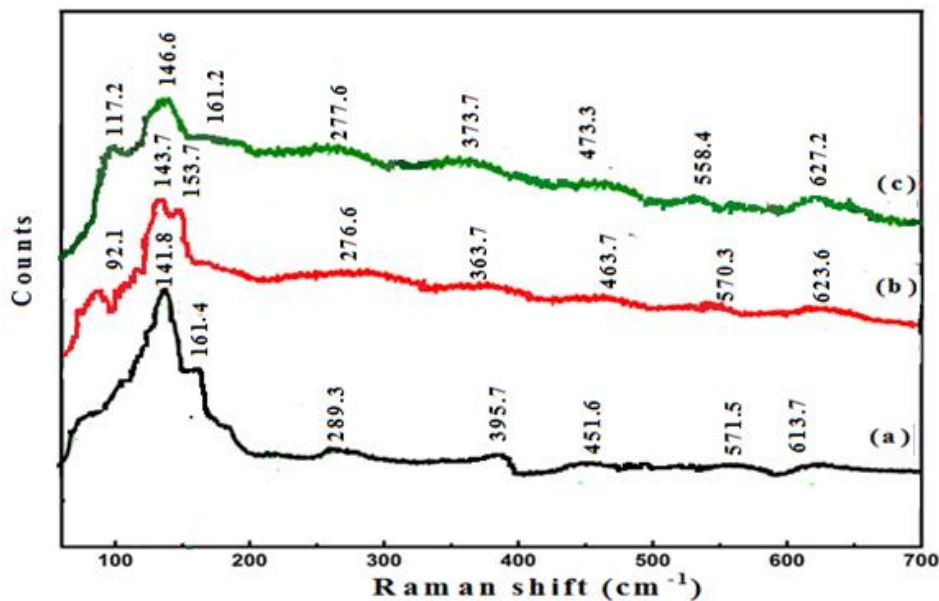


Figure 4: Raman spectra of (a) BEFO (b) BEFMO-1 (c) BEFMO-2 nanocomposites

Table 2: Comparison of E-mode intensities:

Modes	Intensity		
	BEFO	BEFMO –1	BEFMO –2
E7	190	500	840
E8	210	510	520
E9	200	530	610

3.5 SEM analysis

The SEM images of BEFO, BEFMO–1 and BEFMO–2 nanocomposites are shown in Figure 5 (a), (b) and (c) respectively. The morphology of the synthesized nanocomposites showed the agglomerated spherical shape and the size of composites has been diminished by dopants, due to the oxygen vacancies, which slows down the motion of oxygen ion and hence lowers the grain growth [13]. The addition of Mg in BEFO results in inhibition of grain growth, which attributes the reduction in oxygen vacancies in the nanocomposite samples.

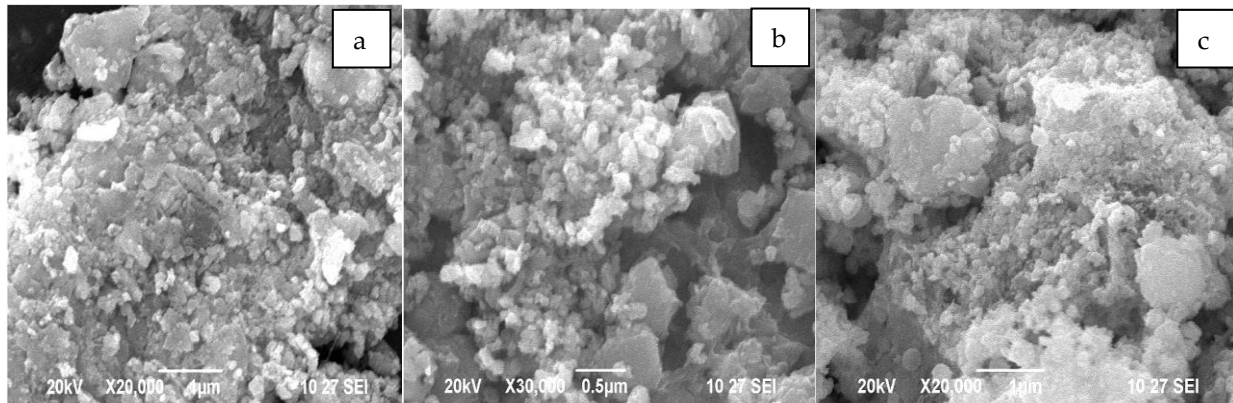


Figure: 5 SEM images of (a) BEFO (b) BEFMO–1 (c) BEFMO–2

3.6 Photoluminescence Studies

The Photoluminescence spectra of Er and Mg doped nanocomposites are shown in Figure 6. The peak appeared in the range of 410 to 450 nm which centered at 416 nm (2.97 eV) and 440 nm (2.81 eV), both are in Visible luminescence region. The strong blue emissions appeared since self-activated centers in the synthesized doped BFO nanocomposites. The Er doped composites showed the peak with high intensity, while the intensity decreases for Mg dopants due to the reduction in the density of oxygen vacancies and hence decrease in electron–hole recombination. Also, Mg co–doping causes the blue shift due to the consequence of quantum confinement. Consequently, the reduction in crystallite size and suppression of recombination rate of electron–hole pairs [18] may influence the photocatalytic action of Er and Mg doped BFO nanocomposites.

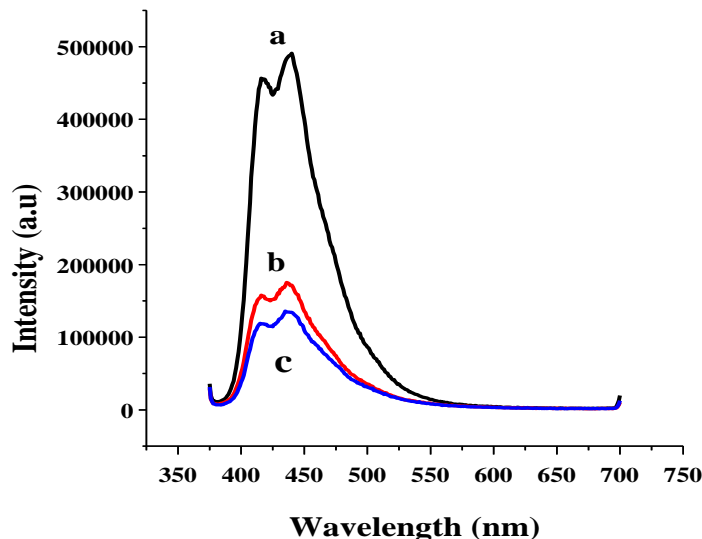


Figure 6: Photoluminescence of (a) BEFO (b) BEFMO –1 (c) BEFMO – 2

3.6 M–H studies

The magnetic behaviours of pure and Erbium doped bismuth ferrite have been investigated by Vibrating Sample Magnetometer at room temperature. The saturation magnetization increases with the increase in concentration of Er^{3+} ions in the BFO samples. This increased saturation magnetization is due to the alignment of spins in the field direction which may cause the decreased particle size. The synthesized

nanoparticles have lesser diameter (~62 nm) of BFO and possess high ferromagnetism, depend on quantum confinement of the particles. The enhanced magnetic parameters (M_s , M_r and H_c) are due to increase in the concentration of Er which causes the structural deformation from rhombohedral to orthorhombic [19].

The room temperature magnetic hysteresis (M–H) of BEFO, BEFMO-1 and BEFMO-2 are shown in Figure: 7 (a), (b) and (c) respectively. The saturation magnetization (M_s) and remanant magnetization (M_r) value of BEFO has been increased in comparison with pure BFO ($M_s = 0.31$ and $M_r = 0.13$) since structural deformation that occurs from rhombohedral to orthorhombic which caused by the addition of Er^{3+} ions. The relative rotation of FeO_6 octahedra takes place in the process of structural transformation from rhombohedral to orthorhombic. Further, the magnetization of BFO has been increased by Mg doped on B site. Both Bi–O and Fe–O bond distance leads to the suppression of spiral spin structure which increases the net magnetization after doping of Mg^{2+} with Er^{3+} . Comparison of magnetic parameters of Pure BFO and doped BFO nanocomposites are shown in table 3.

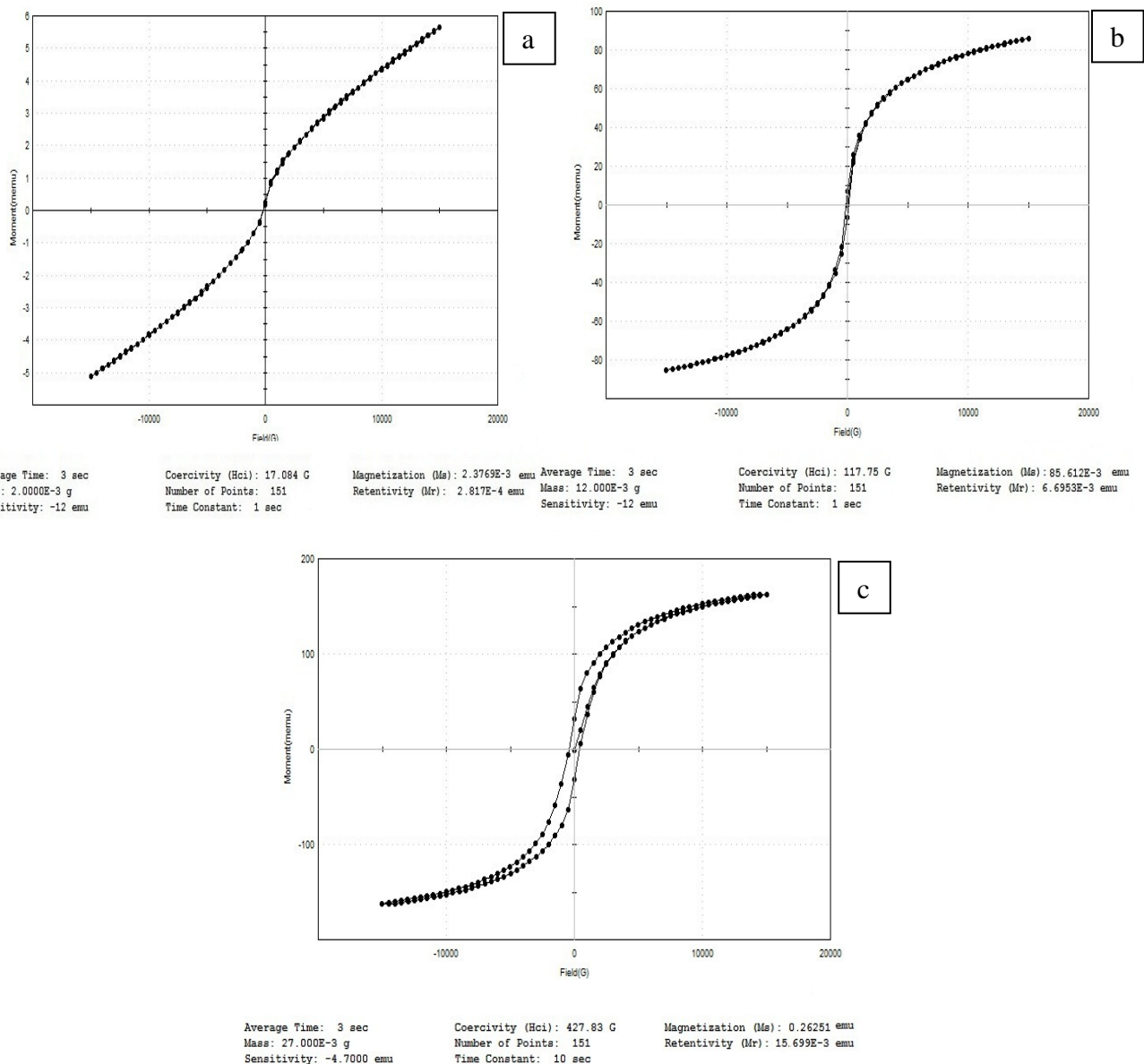


Figure 7: M – H curve of (a) BEFO (b) BEFMO–1 (c) BEFMO–2 at room temperature

Table 3: Comparison of the Magnetic parameters of Pure BFO and Er³⁺ and Mg²⁺ doped BFO nanocomposites:

Compounds	Coercivity (H _c)	Saturation Magnetization (M _s)	Remanent Magnetization (M _r)
BFO	574.6	0.32	0.13
BEFO	17.084	1.1885	0.1408
BEFMO-1	117.5	7.1343	0.5579
BEFMO-2	427.83	9.7223	0.5814

5. Conclusion

The single phase Er³⁺ doped and (Er³⁺, Mg²⁺) co-doped BFO nanocomposites have been synthesized by sol-gel method. UV-Visible and FT-IR spectral analyses confirmed that the dopants Er³⁺ and Mg²⁺ were present in the BFO nanocomposites. From the band gap value, it has been found that doped BFO would be a potential material towards the application of Visible light photocatalyst. XRD and Raman spectra of BFO indicates the structural transformation from rhombohedral to orthorhombic phase and the crystallite size has range of 21–64 nm. The SEM images of Er-doped BFO revealed the spherical shape and the inhibition of grain growth were observed after co-doping. The photoluminescence studies exposed the suppression of recombination rate of electron-hole pairs which supported the enhanced photocatalytic action of BFO nanocomposites. The increased magnetization is due the structural transformation from rhombohedral to orthorhombic and suppression of spiral spin structure which increases the net magnetization after doping of Mg²⁺ and Er³⁺ with BFO.

References

- Priyanka Godara, Ashish Agarwal, Neetu Ahlawat, Sujata Sanghi, Crystal structure, dielectric and magnetic properties of Gd doped BiFeO₃ multiferroics, *Physica B: Condens.*, **2018**, 550, 414-419, <https://doi.org/10.1016/j.physb.2018.08.045>.
- Mukherjee.A, Basu.S, Manna.P.K, Yusuf.S.M, Pal.M, Enhancement of multiferroic properties of nanocrystalline BiFeO₃ powder by Gd-doping, *J. Alloys Compds.*, **2014**, 598, 142-150, <https://doi.org/10.1016/j.jallcom.2014.01.245>.
- XiaYan, Guoqiang Tann, Wenlong Liu, Huijun Ren, Ao Xia, *Ceram. Int.*, **2015**, 41, 3202.
- Wei wei Mao, Xing fu Wang, Yumin Han, Xing'ao Li, Yongtao Li, Yufeng Wang, Yanwen Ma, Xiaomiao Feng, Tao Yang, Jianping Yang, Wei Huang, Effect of Ln (Ln = La, Pr) and Co co-doped on the magnetic and ferroelectric properties of BiFeO₃ nanoparticles, *J. Alloys Compds.*, **2014**, 584, 520–523, <https://doi.org/10.1016/j.jallcom.2013.09.117>.
- Shweta Thakur, Radheshyam Rai, Ashutosh Tiwari, Structural, dielectric and magnetic properties of Gd and Dy doped (Bi_{0.95}RE_{0.05})(Fe_{0.95}Mn_{0.05})O₃ ceramics synthesized by SSR method, *Solid State Commun.*, **2014**, 197, 1–5, <https://doi.org/10.1016/j.ssc.2014.07.024>.
- Vikash Singh, Subhash Sharma, Dwivedi.R.K., Improved dielectric, magnetic and optical properties of Pr and Ti co-substituted BFO ceramics, *J. Alloys Compds.*, **2018**, 747, 611-620, <https://doi.org/10.1016/j.jallcom.2018.02.120>.
- Ahmeda.M.A., Dhahri.E., El-Dek.S. I., Ayoub.M.S., Size confinement and magnetization improvement by La³⁺ doping in BiFeO₃ quantum dots, *Solid State Sci.*, **2013**, 20, 23-28, <https://doi.org/10.1016/j.solidstatesciences.2013.02.023>.

8. Nalwa.K.S., Garg.A., Upadhyaya. A., Effect of samarium doping on the properties of solid-state synthesized multiferroic bismuth ferrite, *Mater. Lett.*, **2008**, 62(6-7), 878-881, <https://doi.org/10.1016/j.matlet.2007.07.002>.
9. Dimple P. Dutta, Tyagi.A.K., Effect of Sm^{3+} and Zr^{4+} codoping on the magnetic, ferroelectric and magnetodielectric properties of sonochemically synthesized BiFeO_3 nanorods, *Appl. Surf. Sci.*, **2018**, 450, 429-440, <https://doi.org/10.1016/j.apsusc.2018.04.202>
10. Xing quan Zhanga, Yu Suia, Xianjie Wanga, Yang Wangc, Zhu Wang, *J. Alloys Compds.*, **2010**, 507.
11. Amit Srivastava, Singh.H.K., Awana.V.P.S., Srivastava.O.N., Enhancement in magnetic and dielectric properties of La and Pr co substituted BiFeO_3 , *J. Alloys Compds.*, **2013**, 552, 336–344, <https://doi.org/10.1016/j.jallcom.2012.09.142>.
12. Prakash Chandra Sati, Manoj Kumar, Sandeep Chhoker, Low temperature ferromagnetic ordering and dielectric properties of $\text{Bi}_{1-x}\text{Dy}_x\text{FeO}_3$ ceramics, *Ceram. Int.*, **2015**, 41(2) Part B, 3227-3236, <https://doi.org/10.1016/j.ceramint.2014.11.012>.
13. Jianlong Xu, Dan Xie, CongYin, Tingting Feng, Xiaowen Zhang, Haiming Zhao, Gang Li, Tian-Ling Ren, Yujie Guan, Xingsen Gao, Wei Pann, Mg-doped $\text{Bi}_{0.8}\text{Ca}_{0.2}\text{FeO}_3$ with enhanced ferromagnetic properties, *Mater. Lett.*, **2014**, 122, 139–142, <https://doi.org/10.1016/j.matlet.2014.01.127>
14. Tiantian Wang, Hongmei Deng, Huiyi Cao, Wenliang Zhou. Guoen Weng, Shaoqiang Chen, Pingxiong Yang, Junhao Chu, Structural, optical and magnetic modulation in Mn and Mg co-doped BiFeO_3 films grown on Si substrates, *Mater. Lett.*, **2017**, 199, 116 -119, <https://doi.org/10.1016/j.matlet.2017.04.068>
15. Yumin Hana, Weiwei Mao, Chuye Quana, Xingfu Wang, Jianping Yang, Tao Yanga, Xing'ao Li, Wei Huang, *Mater. Sci. Eng. B: Solid State Mater. Adv. Technol.*, **2014**, 188, 26.
16. Yinina Ma, Wenyu Xing, Jieyu Chen, Yulong Bai, Shifeng Zhao, Hao Zhang, The influence of Er, Ti co-doping on the multiferroic properties of BiFeO_3 thin films, *Appl. Phys. A*, **2016**, 122(2), 63. <http://doi.10.1007/s00339-016-9628-3>.
17. Yilin Zhang, Yuhan Wang, Ji Qi, Yu Tian, Mingjie Sun , Junkai Zhang , Tingjing Hu , Maobin Wei , Yanqing Liu, Jinghai Yang, Enhanced Magnetic Properties of BiFeO_3 Thin Films by Doping: Analysis of Structure and Morphology, *Nanomaterials*, 2018, 8, 711. <http://doi:10.3390/nano8090711>
18. Jyoti Sharma, Deepak Basandrai, Srivastava.A.K., Ce–Co-doped BiFeO_3 multiferroic for optoelectronic and photovoltaic applications, *Chin.phys. B*, **2017**, 26, 116201, DOI 10.1088/1674-1056/26/11/116201.
19. Sunil Kumar.K., Ramanadha.M., Sudharani.A., Ramu.S., Vijayalakshmi.R.P., Structural, Magnetic and Photoluminescence properties of BiFeO_3 : Er-Doped Nanoparticles prepared by Sol-Gel Technique, *J. Supercond. Nov. Magn.*, **2019**, 32, 1035-1042, <https://doi.org/10.1007/s10948-018-4789-2>.